Possible effects of tectonic shear strain on phyllosilicates : a case study from the Kandersteg area, Helvetic domain, Central Alps, Switzerland

Autor(en): **Árkai, Péter / Ferreiro Mählmann, Rafael / Suchý, Václav**

Objekttyp: **Article**

Zeitschrift: **Schweizerische mineralogische und petrographische Mitteilungen = Bulletin suisse de minéralogie et pétrographie**

Band (Jahr): **82 (2002)**

Heft 2: **Diagenesis and Low-Grade Metamorphism**

PDF erstellt am: **21.09.2024**

Persistenter Link: https://doi.org/10.5169/seals-62365

SCHWEIZ. MINERAL. PETROGR. MITT. 82, 273–290, 2002

Possible effects of tectonic shear strain on phyllosilicates: a case study from the Kandersteg area, Helvetic domain, Central Alps, Switzerland

by *Péter Árkai*[1], *Rafael Ferreiro Mählmann*[2], *Václav Suchý*[3], *Kadosa Balogh*[4], *Ivana Sýkorová*[5] and *Martin Frey*[2†]

Abstract

Relatively few and rather controversial data exist on the effects of tectonic shear strain on phyllosilicate properties under conditions of incipient metamorphism. In the present paper, X-ray powder diffractometric illite and chlorite "crystallinity", apparent mean crystallite thickness and lattice strain data are provided from a shale–slate–mylonitized slate sample series. These results are compared with published and new organic petrographic data and microstructural observations. The sample series represents a characteristic vertical section from the Helvetic domain (Central Alps, Switzerland). From top the bottom, this section crosses the boundaries between the Wildhorn nappe, the Gellihorn nappe, and the Doldenhorn nappe.

The diagenetic/metamorphic grade increases downwards, as shown by phyllosilicate characteristics: Mainly diagenetic conditions prevail in the Wildhorn, partly diagenetic, partly anchizonal conditions in the Gellihorn, and mostly anchizonal conditions in the studied part of the Doldenhorn nappe. This pattern confirms the previously published trend for the Helvetic domain in general. Compared with the retarded phyllosilicate reaction progress, high grades of coalification, expressed in vitrinite reflectance and graphitization data, are demonstrated throughout the profile. Most probably, this discrepancy can be attributed to differences in kinetic factors influencing metamorphism of phyllosilicates and coalified organic matter during the relatively short-term regional heating. A local, but systematic increase in metamorphic grade in the vicinity of nappe boundaries and also within each nappe, marked by a decrease in "crystallinity" values of clay-size phyllosilicates suggests that high tectonic shear strain enhanced phyllosilicate reaction progress. High tectonic strain near the thrust planes has been well established also by the occurrence of highly coalified organic particles and by the development of graphitized organic matter. In addition to shear-strain, migration of fluids also affected the phyllosilicates, especially in the lower, cataclastic-mylonitic zone of the Gellihorn nappe. K–Ar dates obtained on the 0.1–2 μm illite-muscovite-rich fraction samples indicate incomplete, partial rejuvenation in the low anchizonal part of the Wildhorn nappe and in the low to high anchizonal parts of the Gellihorn nappe, but almost complete resetting in the anchizonal Doldenhorn nappe.

Keywords: phyllosilicate "crystallinity", coal petrographic parameters, K–Ar geochronology, tectonic strain, low-temperature metamorphism, Central Alps.

Introduction

Laboratory experiments at low pressure and temperature, equivalent to high diagenetic and very low-grade metamorphic conditions, have provided no direct evidence on the relationship between tectonic shear strain and phyllosilicate reaction progress. Our present knowledge on these effects has been accumulated in case studies carried out in fold and thrust belts, at scales ranging from microscopic to regional (for reviews and comprehensive studies read FREY, 1987; KISCH, 1989;

[1] Laboratory for Geochemical Research, Hungarian Academy of Sciences, Budaörsi út 45, H-1112 Budapest, Hungary. <arkai@geochem.hu>

[2] Mineralogisch-Petrographisches Institut der Universität, Bernoullistrasse 30, CH-4056 Basel, Switzerland.

[3] Geological Institute, Academy of Sciences of the Czech Republic, Rozvojová 135, 165 00 Prague 6-Suchdol, Czech Republic. Present address: National Technical Museum, Kostelni 42, 170 78 Prague 7, Czech Republic.

[4] Institute of Nuclear Research, Hungarian Academy of Sciences, Bem tér 18/c, H-4001 Debrecen, Hungary.

[5] Institute of Rock Structure and Mechanics, Academy of Sciences of the Czech Republic, V Holešovičkách 41, 182 09 Prague 8, Czech Republic.

† Martin Frey died in an accident in the Swiss Alps.

1991; WARR et al., 1996; ÁRKAI et al., 1997; MERRIMAN and FREY, 1999). Recently, BURKHARD and BADERTSCHER (2001) found that directly measured finite tectonic strain had no influence on illite "crystallinity" (KI) of Eocene limestone breccias from the Swiss Alps. BURKHARD and GOY-EGGENBERGER (2001) concluded that the close correlation between KI and tectonic strain intensity "should not be used to infer that KI values depend on strain intensity. Rather, both strain intensity and KI are strongly dependent on temperature." Controversial opinions have been presented on the behaviour of illite-muscovite and chlorite, expressed by changes in phyllosilicate "crystallinity", mean crystallite thickness (size) and lattice strain, as a function of varying tectonic strain. It is evident that the response of phyllosilicates to increasing strain depends on numerous physical and chemical factors during and following deformation and (re)crystallization (for comprehensive reviews see ÁRKAI et al., 1997 and MERRIMAN and PEACOR, 1999). Such factors may include the strain, the temperature of the rock before, during and after deformation, the fluid/rock ratio, the migration of fluids, the relative timing of deformation and (re)crystallization, and the modal composition, as well as the physical differences between the phyllosilicates in question and their surrounding mineral phases.

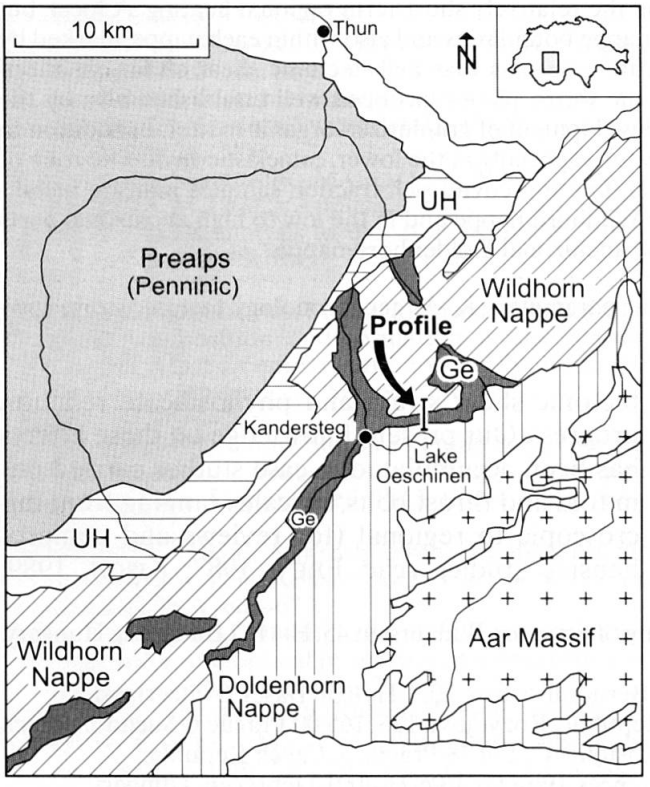

Fig. 1 Geological map of the Kandersteg area, Central Alps with inset showing the location of the area in Switzerland. Ge = Gellihorn nappe, UH = Ultrahelvetic units.

The present paper provides new illite and chlorite "crystallinity", apparent mean crystallite thickness and lattice strain data from a partly mylonitized shale/slate series representing a profile that crosses two thrust planes in the Helvetic domain of the Swiss Central Alps. Phyllosilicate parameters are compared with microstructural features and coal petrographic characteristics of the dispersed organic matter.

Geological setting

The investigated steep profile represents some 1100 m difference in altitude and is located in central Switzerland, east of the village of Kandersteg, directly north of Lake Oeschinen (Fig. 1). This profile crosses three nappes, namely (from top to bottom) the Wildhorn, Gellihorn and Doldenhorn nappes; these build up the northern marginal Helvetic domain of the Central Alps. The stratigraphic age of the sequences ranges from Liassic to Eocene. Jurassic and Cretaceous limestones and marls and also the Eocene sandstones are interbedded with shales (TRÜMPY, 1980; BURKHARD, 1988). The Gellihorn nappe also contains the Taveyannaz series described by ZWAHLEN (1986, 1993). During the Alpine collision the Penninic nappes were thrusted onto the Helvetic nappe edifice, causing considerable burial, deformation and metamorphism up to lower greenschist facies conditions. According to FREY et al. (1980) and FREY and FERREIRO MÄHLMANN (1999) the grade of orogenic metamorphism generally increases from structurally higher to lower units and from external (northwestern) to internal (southeastern) parts within the same tectonic unit in the Helvetic domain. In the vicinity of the profile studied, high diagenetic conditions were determined for the Wildhorn nappe, while anchizonal conditions (more or less equivalent to the prehnite-pumpellyite facies, see FREY, 1986; FERREIRO MÄHLMANN, 1996) were found in the Gellihorn and Doldenhorn nappes. Chronostratigraphic, structural, isotope geochronological data, and results of thermal modeling of organic maturity show that temperature-dominated metamorphism prevailed, with peak conditions between 34 and 30 Ma (see BURKHARD, 1988; HUON et al., 1994; ERDELBROCK, 1994; RAHN et al., 1995, 1997). The main cleavage formation and foliation at nappe thrusts started slightly earlier, i.e. 36 to 30 Ma ("Calanda phase"), with an older foliation ("Pizol phase") being overgrown by metamorphic minerals in some places of the Helvetic domain. The tectono-metamorphic evolution of the Kandersteg area is rather similar to that of the

Glarus Alps (HUNZIKER et al., 1986). Younger ages in the west of the Helvetic domain are due to the propagation of the deformational and metamorphic front to the north, involving also the lower structural units of the Ultrahelvetic domain (PFIFFNER, 1986). Greenschist facies areas cooled down below 300 to 250 °C between 25 and 22 Ma (Meinert Rahn, personal comm., unpubl. zircon fission track data). Organic maturity models using the evolution model of PFIFFNER (1986) also indicate a relatively short effective heating interval (RAHN et al., 1994), i.e. the time period of near-peak metamorphic conditions. A time span of 2 to 5 Ma is empiricaly deduced from the organic maturity models.

Methods

For illite and chlorite "crystallinity" and vitrinite reflectance (VR) studies, dark gray to black silty shales, shaly siltstones (with various amounts of carbonate and detrital quartz material) and their metamorphic equivalents, namely slates and mylonitized slates were selected. In addition, several samples of sandstone (greywacke) and marly slate and limestone have also been investigated. The procedure of preparing 0.1–2 μm grain-size fraction samples was similar to that used by KÜBLER (1968), as described by FREY (1988). Procedures and instrumental conditions applied in XRD work were those described in detail by ÁRKAI et al. (1997).

The Kübler index (KI) of illite-muscovite, often termed illite "crystallinity", represents the calibrated full-width-at-half-maximum (FWHM) of the first, 10-Å basal reflection of illite-muscovite. Chlorite "crystallinity" indices, indicated as ChC(001) and ChC(002) in the present paper, express the FWHM values of the first (14-Å) and second (7-Å) basal reflections of chlorite. Relative standard deviation of the FWHM measurements is 3.2% (e.g., the standard deviation of KI = 0.220 is $s = 0.007$ $\Delta°2\theta$). The actual boundary ranges of KÜBLER's anchizone are KI = 0.25–0.42 $\Delta°2\theta$. Correlation with the KI gives calculated boundary values of the anchizone for the ChC(001) = 0.26–0.37 $\Delta°2\theta$ and ChC(002) = 0.24–0.30 $\Delta°2\theta$, respectively (see also ÁRKAI et al., 1995b). All of these boundary values refer to air-dried (AD) mounts.

The apparent mean crystallite thickness and lattice strain of illite-muscovite and chlorite were calculated from line-profiles of the first order (10-Å), those of chlorite from line profiles of the second (7-Å) XRD basal reflections, based on the Voigt method of LANGFORD (1978), as modified in the Philips APD-1700 software package. This method is also called single-line Fourier analysis. Details of these calculations as well as the results of a comprehensive study and assessment of available XRD-based methods for calculating crystallite size and lattice strain were given by ÁRKAI et al. (1996, 1997). Relative standard deviations of the mean crystallite thickness and lattice strain calculations vary between 4 and 10% (e.g., for a mean crystallite size value of 686 Å, $s = 33$ Å, and for a mean lattice strain of 0.71% $s = 0.06\%$, when $n = 15$).

The coal petrographic results follow SUCHÝ et al. (1997), whose organic petrography data set has been completed by measurements on new samples using a UMSP 30-Petro (Opton – Karl Zeiss) reflected light microscope. Reflectance measurements were calibrated using zirconia (R = 3.125%) and diamond (R = 5.1%) as optical standards. Arithmetic means of maximum and minimum reflectance (R_{max}, R_{min}) and bireflectance (ΔR) values of vitrinite were used for comparison.

Analytical procedures applied for K–Ar dating of illite-muscovite-rich, clay-size fractions were those described by ÁRKAI et al. (1995a).

Results

ROCK TYPES AND THEIR DEFORMATION

Rock types, the intensity of their tectonic (shear) deformation, and the sampling altitude of all specimens are summarized in Table 1. After SUCHÝ et al. (1997) the qualitative categories are characterized by the following main features of rock deformation:

– *none:* compactional, burial-related grain-to-grain contacts;

– *weak:* thin shear zones developed;

– *moderate:* development of shear zones in pelitic layers, and some "barbed" quartz grains in silty lithologies, brittle-ductile deformation transition of calcite-quartz fabrics;

– *strong:* intense shear, viscous grain-boundary sliding in quartz grains; development of dislocation creep (weaker, protomylonitic phase), plain penetrative cleavage formation;

– *very strong:* mylonitic fabrics, "ribbon quartz", dynamic recrystallization and development of subgrain boundaries in quartz. Embryonal forms of crenulation cleavage are also found in quartz – white mica-rich parts, where the initial cleavage formation was overprinted by the main cleavage phase during peak metamorphism.

In general, the intensity of tectonic (shear) deformation increases downwards in the profile. The

nappe boundaries are characterized by strong to very strong deformation. However, strong tectonic shear was not concentrated and restricted to the nappe boundaries. Strongly sheared rocks were observed also within the rock sequences of the Gellihorn and Doldenhorn nappes. Strong deformation is restricted to incompetent layers (shales, slates) and is typically associated to Helvetic multilayer folds. Flexural slip folds with crystal fibres and en échelon tension gashes formed by layer-parallel shear during flexural slip folding are common. The boundary between the Gellihorn and Doldenhorn nappes is a complex, ca. 50 m thick zone built up by Tertiary slates intercalated with 2 to 8 m thick limestone layers. The upper limit of this zone is indicated in Figs. 2 to 5 by a dotted line within the Gellihorn nappe.

MODAL COMPOSITION

Modal compositions of the "clay fraction" samples are given in Table 2 (abbreviations of mineral names from BUCHER and FREY, 1994). Illite-muscovite and chlorite predominate in the whole profile investigated. Quartz always occurs in subordinate amounts, while pyrite is the characteristic opaque mineral indicating a reducing environment. Weak XRD traces of paragonite or margarite and mixed K–Na-rich mica were detected in a few samples.

Considering the relative abundances of the two main phyllosilicates, the following systematic changes were observed in the profile. Illite-muscovite is dominant in the main parts of the Wildhorn and the Doldenhorn nappes. In contrast, chlorite predominates in the Gellihorn nappe as well as in the lower- and uppermost parts of the Wildhorn and Doldenhorn nappes that border the Gellihorn nappe. As chlorite becomes more abundant than illite-muscovite, the albite content also increases. In one sample (MF-2758) illite-muscovite is subordinate and stilpnomelane occurs. At least two more or less complementary models may be set up to explain these changes in modal composition. Variations in the illite-muscovite/chlorite ratio, abundance of albite, and perhaps the sporadic occurrence of stilpnomelane

Table 1 Rock types and intensity of their tectonic deformation.

No. of sample	m (a.s.l.)	rock type	intensity of deformation
MF-2719	2645	shale to slate with silty laminae	none to weak
MF-2720	2600	shale to slate with silty laminae	weak
MF-2721	2485	calcareous shale - clayey limestone	weak
MF-2722	2420	silty shale to slate	weak to moderate
MF-2723	2375	silty shale to slate	moderate to strong
MF-2724	2215	siltstone	moderate
MF-2725	2140	mylonitized siltstone with minor clay partings	strong
MF-2725a	2140	mylonitized siltstone with minor clay partings	moderate to strong
MF-2726	2100	metasandstone (-graywacke)	moderate
MF-2727	2100	siltstone with subordinate clay partings	strong
MF-2728	2100	metasandstone (-graywacke)	moderate
MF-2729	2075	siltstone with subordinate clay partings	strong
MF-2753	2045	slate with silty partings	very strong
MF-3178	2030.3	marly slate with calcitic partings	moderate
MF-3179	2030	marly slate	moderate to strong
MF-2754	2025	slate with silty partings	very strong
MF-3180	2020	marly slate	weak to moderate
MF-3181	2015.2	marly slate	strong
MF-3182	2015	clayey, recrystallized, stylolitic limestone	moderate to strong
MF-3183	2000	marly slate with calcitic partings	strong
MF-2755	1990	mylonitized slate with quartzitic partings	very strong
MF-2756	1990	mylonitized slate with quartzitic partings	very strong
MF-2757	1945	metasiltstone with clayey partings	moderate
MF-2757a	1945	sandstone, clay matrix with quarzitic partings	moderate to strong
MF-2757b	1945	mica-organic matter pressure solution layer	strong
MF-2758	1890	metasandstone (-graywacke)	moderate
MF-2760	1870	strongly recrystallized metasiltstone	strong
MF-2761	1700	strongly recrystallized metasiltstone (clayey)	strong
MF-2762	1635	slate with mylonitized quartz partings	very strong

may be related to an enrichment in volcanogenic fine-clastic material of basic-intermediate composition in the Gellihorn nappe and in certain parts of the Doldenhorn nappe as compared to the Wildhorn nappe. Alternatively, fluid-controlled chloritization (and albite formation) along fault zones may have played a role.

PHYLLOSILICATE "CRYSTALLINITY"

Illite and chlorite "crystallinity" values in relation to altitude and structural location are given in Table 3 and shown in Fig. 2.

The investigated part of the Wildhorn nappe experienced diagenetic conditions. KI values decrease irregularly downwards, reaching the low-T part of the anchizone near the thrust boundary. The ChC values, characteristic mostly of high diagenesis, show strong variations.

In the Gellihorn nappe, fluctuations in KI and ChC are strong within the whole ca. 140 m thick section. Low to high anchizonal KI and ChC values were observed near the upper and lower nappe boundaries, while most of the samples from the middle part of the Gellihorn nappe reflect only diagenetic conditions. Near the upper boundary of the Gellihorn nappe, the differences between ChC(001) values measured on air-dried and glycolated mounts are large, indicating the presence of swelling interstratifications in chlorite.

KI data of the uppermost part of the Doldenhorn nappe show a strong decrease followed by a moderate increase downwards from ca. 1900 to 1600 m. In contrast, ChC indices show only irregular fluctuations. Except the near-thrust (uppermost) samples of this nappe, which fall into the zone of high diagenesis, most of the KI data indicate anchizonal conditions, in accordance with the ChC values.

APPARENT MEAN CRYSTALLITE THICKNESS AND APPARENT MEAN LATTICE STRAIN

As calculated from the 10-Å basal reflection of illite-muscovite, a stepwise increase in apparent mean crystallite thickness and a decrease in ap-

Table 2 Modal composition of the 0.1–2μm grain-size fractions determined by XRD (abbreviations of mineral names after BUCHER and FREY, 1994).

sample MF-	altitude (m, a.s.l.)	Ill-Ms	Chl	Pg or Mrg	Pg/Ms	Qtz	Ab	Kfs and/or Rt	Py	Stp	Gt
2719	2645	+	x	tr?		0					
2720	2600	+	x			0					
2721	2485	+	0			0			tr		
2722	2420	+	x	tr?		0	tr?				
2723	2375	+	x			0			tr		
2724	2215	+	0			0			tr		
2725	2140	x	+			0	tr?				
2726	2100	0	+			0	0	tr			
2727	2100	x	+			0	0		tr		
2728	2100		+			0	0	0			
2729	2075	x	x			0	tr?				
2753	2045	x	x			0	0				
3178	2030.3	+	x		tr?	0					
3179	2030	x	x			0	0				
2754	2025	x	+	tr?		0	0		tr		
3180	2020	x	x			0					
3181	2015.2	x	x		tr?	0	0	tr?			
3182	2015	+	x	tr?	tr?	0	0	tr?	tr		
3183	2000	x	x		tr?	0		tr?			
2755	1990	x	+			0	0	0	tr		
2756	1990	x	x			0	0	tr?	tr		
2757	1945	+	x	tr?		0	tr?	tr?	tr		
2758	1890	0	+			0				0	
2760	1890	+	0			0			tr		tr?
2761	1700	+	x		tr?	0			tr		tr?
2762	1635	+	x			0		tr?	tr		

Legend: + dominant x significant 0 subordinate tr traces ? questionable

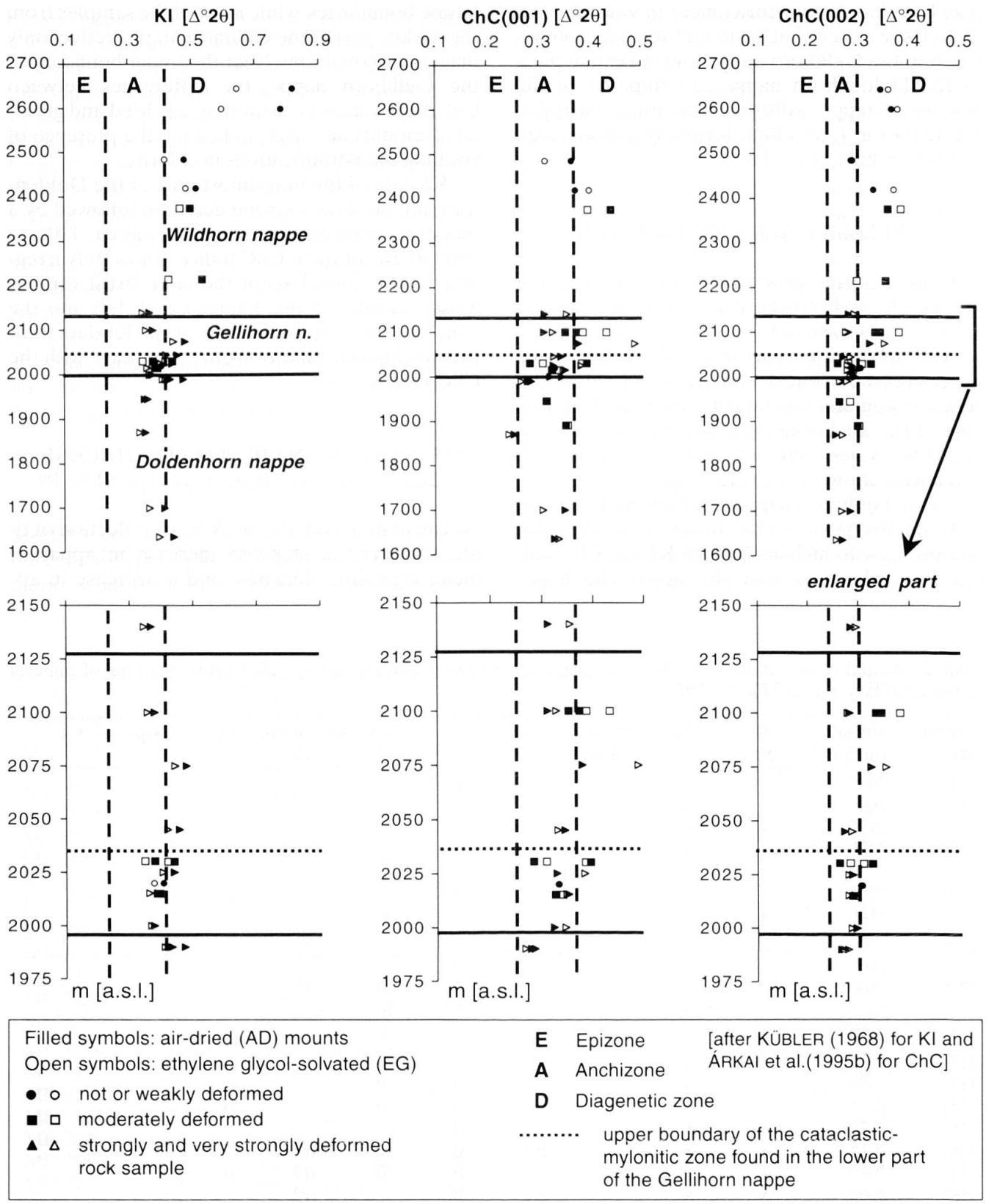

Fig. 2 Variations in KI and ChC values (expressed in Δ°2θ) along the profile crossing the nappe boundaries.

parent mean lattice strain are observable downwards to the lower boundary of the Wildhorn nappe (Fig. 3). The maximum mean crystallite thickness is found at the boundary, while the minimum mean lattice strain is found some 70 m above the thrust plane. In the Gellihorn nappe, an increase in mean crystallite thickness and a decrease in mean lattice strain are indicated towards the upper nappe boundary. Similar general trends are valid also towards the lower nappe boundary,

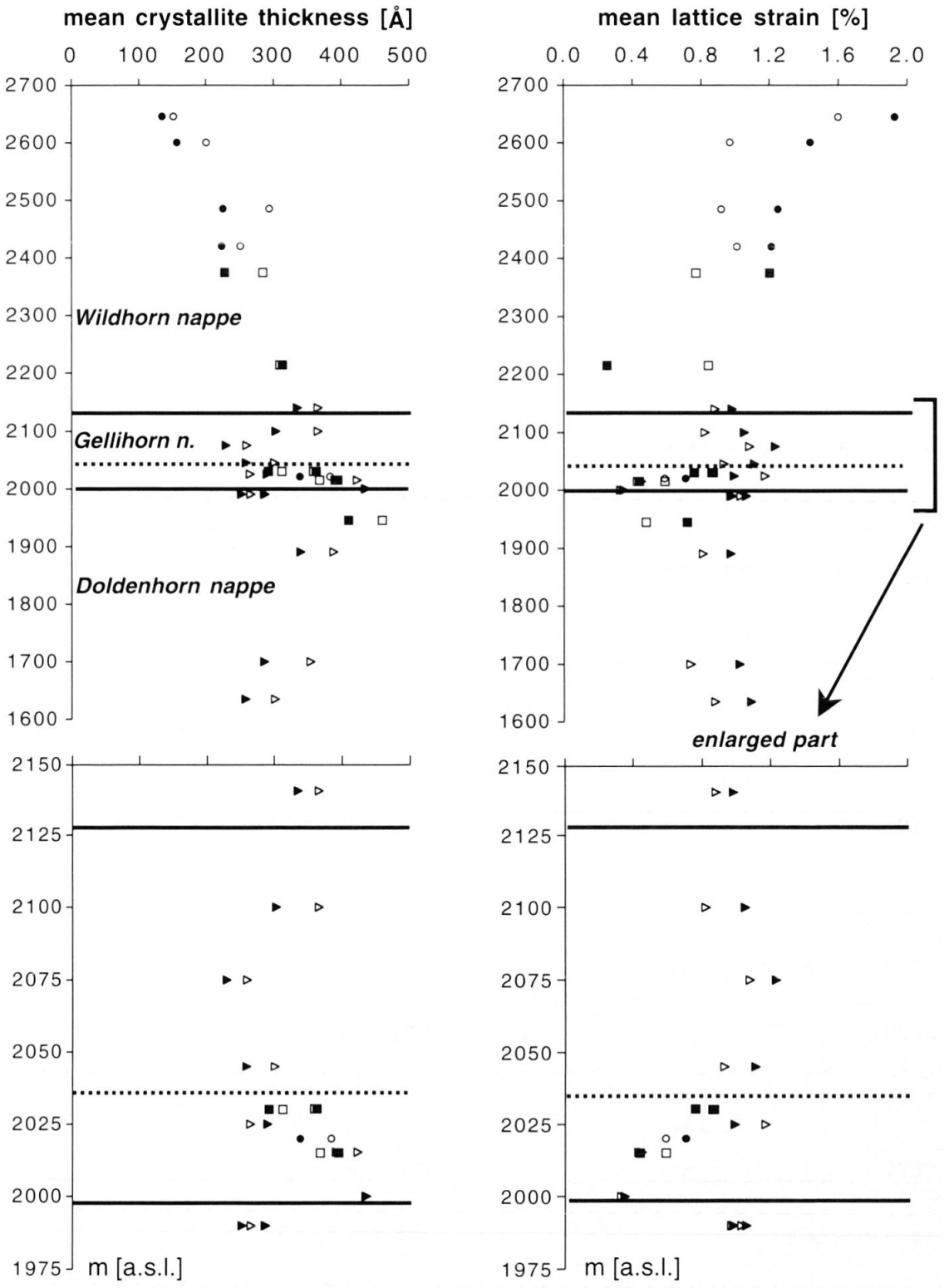

Fig. 3 Changes in apparent mean crystallite thickness and mean lattice strain values of illite-muscovite calculated from the 10-Å reflections. Symbols as in Fig. 2.

although in the lower, ca. 50 m thick cataclastic to mylonitic zone above the basal thrust plane the scatter of the values is rather strong. The topmost sample, from near the thrust of the Doldenhorn nappe, differs in lower mean crystallite thickness and higher mean lattice strain values from the underlying samples; the latter show a downward decrease in mean crystallite thickness and an increase in mean lattice strain.

Using the 7-Å reflection of chlorite (Fig. 4), mean crystallite thickness and mean lattice strain data were obtained for the whole geological pro-

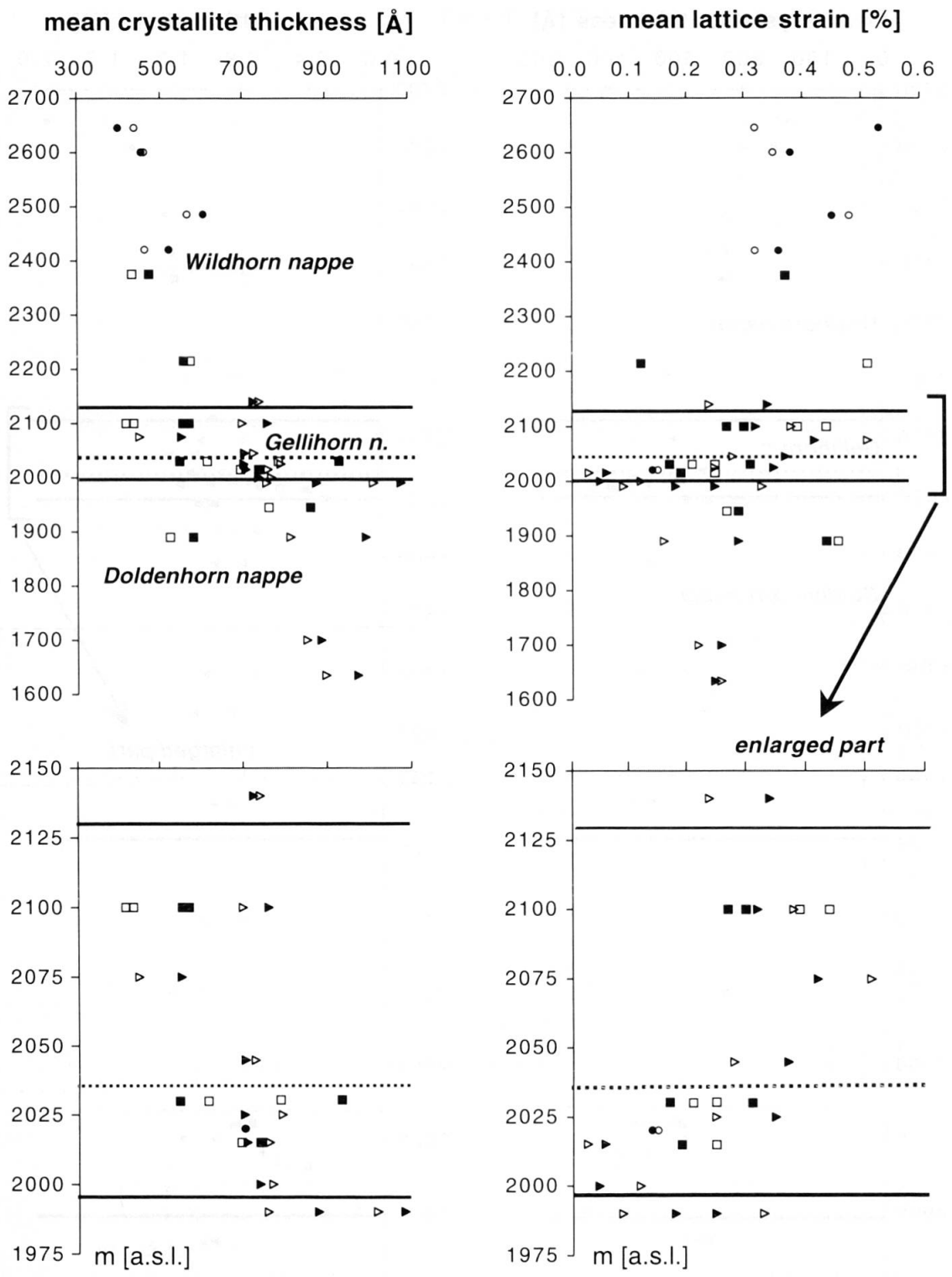

Fig. 4 Apparent mean crystallite thickness and mean lattice strain of chlorite calculated from the 7-Å reflection. Symbols as in Fig. 2.

file. Trends in these, observed in the Wildhorn nappe, are similar to those described for illite-muscovite, although the fluctuations are larger for chlorite. In the Gellihorn nappe, chlorite mean crystallite thickness values scatter strongly, and mean lattice strain values decrease downwards. In general, the mean crystallite thickness values of chlorite in the Doldenhorn nappe are larger than those in the two overlying nappes, while the mean lattice strain values are practically the same as in the Gellihorn nappe. In the Doldenhorn nappe, large fluctuations in mean crystallite thickness are characteristic, especially above 1900 m a.s.l.

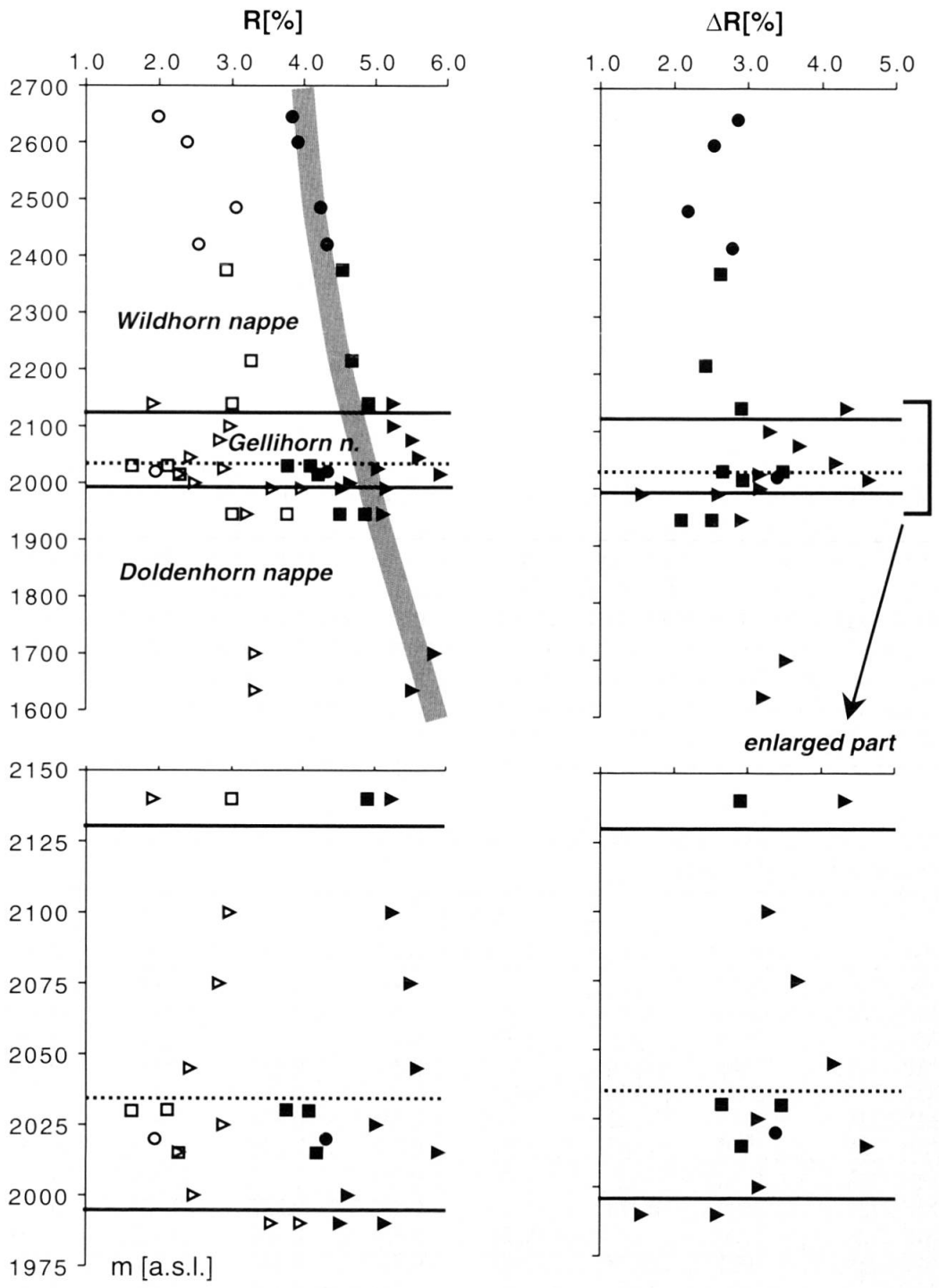

Fig. 5 Variations in vitrinite reflectance along the Kandersteg profile. In the left column filled symbols = R_{max}, open symbols = R_{min}. Other symbols correspond to Fig. 2. The bold gray line represents the result of thermal modeling (see text).

MATURITY OF DISPERSED COALIFIED ORGANIC MATTER

Table 4 summarizes the organic petrographic data available and obtained on the sample series. A continuous increase in R_{max} and fluctuations in R_{min} and ΔR downwards in the Wildhorn nappe are found (Fig. 5). The highest R_{max} and ΔR and the lowest R_{min} values were obtained just above the nappe boundary. Within the Gellihorn nappe, a slight downward increase in R_{max} and ΔR, and a decrease in R_{min} are seen, whereas strong, irregular fluctuations of VR values occur in the lower, ca. 50 m thick cataclastic to mylonitic zone at the base of the Gellihorn nappe. The strongest variation in the R_{max}, ΔR and R_{min} values is found in this narrow part of the profile. In the underlying Doldenhorn nappe, R_{max} and ΔR increase and

R_{min} decreases downwards, with slightly scattering values.

In the Kandersteg profile the first appearance of a fine, needle-like graphitic material is restricted to narrow micro-shear zones. Graphitization begins with the onset of viscous grain-boundary sliding and the development of dislocation creep (weaker mylonitic phase). In between micro-shear zones, however, the rock matrix escaped intense shearing, and vitrinite grains of lower reflectance and bireflectance are found there. For example, reflectance of the dispersed organic matter in the sheared sample MF2757 shows a trimodal distribution (Fig. 6). Group 1 represents vitrinite particles reflecting their metamorphic grade. Group 2 is identical in organic material to Group 1, but derives from the strongly deformed part of the sample, where vitrinite reflectance is enhanced due to pre-graphitic structures. In particles of Group 2 lamellae of variably reflecting, <1.5 μm thick layers lie in the main foliation. These differences in organic maturity refer to micro-scale variations and localization of tectonic strain that caused enhanced VR in the strongly deformed micro-domains of the rocks. In both sections detrital material of the semi-graphite to graphite stages (Group 3) was found (optical graphite). In section MF2757b, "graphite" is accumulated in the shear zone and behaves like newly formed vitrinite of the graphite stage. However, the trimodal distribution clearly points to its detrital origin.

In other samples (e.g., MF2756, 3178, 3179, 3180 and 3182), lower R_{max} and ΔR values may be due to solid, homogeneous bituminite, formed during the last tectonic movements that caused crenulation of the older foliation, and migration of fluid hydrocarbons. The late stage of migration during the cooling path of the metamorphic history is documented by relatively low maturity.

Thermal modeling of the organic maturity data of SUCHÝ et al. (1997) was attempted using the VR model "EASY%R_o" of SWEENEY and BURNHAM (1990) and the commercial maturity simulation package "PDI/PC 2.2-1D" (IES GmbH Jülich, Germany). We modeled the pre-orogenic burial history and the metamorphic history following basin inversion and nappe thrusting, as outlined by FERREIRO MÄHLMANN (2001). For the pre-orogenic history a temperature gradi-

Table 3 Illite and chlorite "crystallinity" values (KI and ChC, expressed in $\Delta°2\theta$) of the 0.1–2 μm grain-size fraction samples.

	m	air-dried mounts			glycolated mounts		
No. of sample	(a.s.l.)	KI	ChC(001)	ChC(002)	KI	ChC(001)	ChC(002)
MF-2719	2645	0.817	–	0.346	0.642	0.441	0.361
MF-2720	2600	0.781	–	0.367	0.595	–	0.379
MF-2721	2485	0.476	0.363	0.291	0.415	0.312	0.289
MF-2722	2420	0.514	0.371	0.332	0.482	0.398	0.371
MF-2723	2375	0.495	0.441	0.360	0.463	0.396	0.386
MF-2724	2215	0.532	–	0.356	0.428	–	0.300
MF-2725	2140	0.367	0.311	0.285	0.346	0.355	0.296
MF-2726	2100	–	0.373	0.345	–	0.386	0.381
MF-2727	2100	0.378	0.310	0.283	0.357	0.327	0.279
MF-2728	2100	–	0.351	0.335	0.309	0.432	0.381
MF-2729	2075	0.478	0.378	0.325	0.442	0.488	0.354
MF-2753	2045	0.455	0.344	0.274	0.419	0.330	0.288
MF-3178	2030.3	0.378	0.282	0.263	0.347	0.308	0.284
MF-3179	2030	0.438	0.394	0.328	0.418	0.384	0.310
MF-2754	2025	0.438	0.328	0.289	0.404	0.383	0.282
MF-3180	2020	0.403	0.330	0.304	0.375	0.331	0.307
MF-3181	2015.2	0.388	0.351	0.293	0.361	0.348	0.282
MF-3182	2015	0.393	0.325	0.289	0.386	0.339	0.292
MF-3183	2000	0.377	0.322	0.297	0.368	0.345	0.288
MF-2755	1990	0.472	0.278	0.268	0.418	0.266	0.267
MF-2756	1990	0.431	0.285	0.273	0.409	0.284	0.281
MF-2757	1945	0.352	0.314	0.266	0.362	0.315	0.287
MF-2758	1890	–	0.352	0.301	–	0.357	0.304
MF-2760	1870	0.356	0.252	0.258	0.337	0.242	0.272
MF-2761	1700	0.414	0.350	0.287	0.368	0.308	0.270
MF-2762	1635	0.443	0.329	0.271	0.398	0.338	0.259

ent of 30°C km^{-1}, and for the orogenic history a slightly enhanced gradient (FREY et al., 1976) was used. These methods use a pure conduction model, without considering additional heating effects due to shear (frictional heating) or fluid flow (advective heating). Consequently, enhanced R_{max} values of the strongly deformed samples from the lower part of the Wildhorn nappe and from the Gellihorn nappe were not included in the model, nor were R_{max} values of metabituminite found in the lower part of the Gellihorn nappe. The best approximation was obtained using a time interval

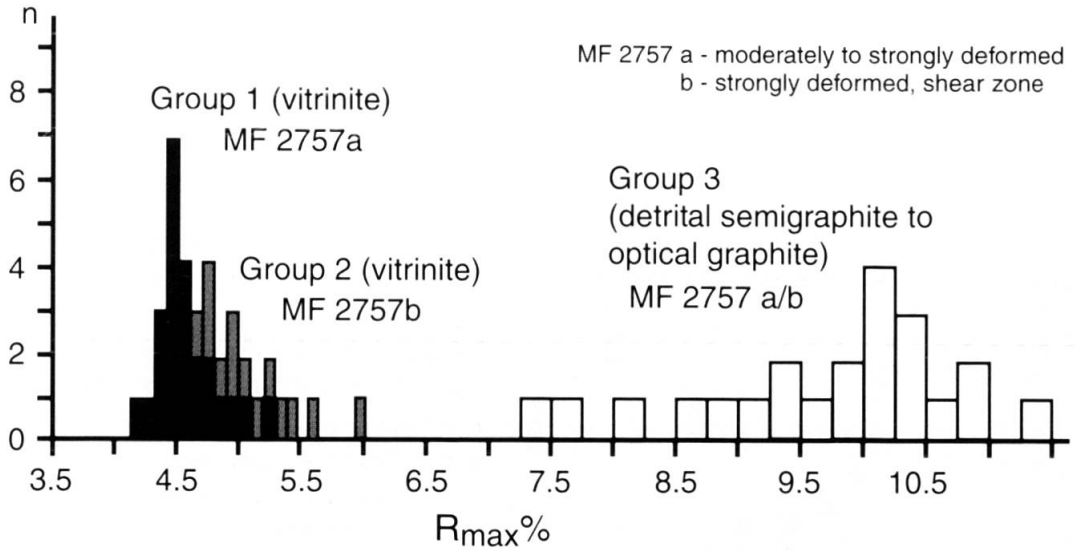

Fig. 6 Trimodal vitrinite reflectance histogram of sample MF 2757. Combined data presented for thin sections a and b. See text for explanation.

Table 4 Vitrinite reflectance data.

No. of sample	m (a.s.l.)	vitrinite reflectance (%)					
		R(max)		R(min)		R	n
		x	s	x	s	x	
MF-2719	2645	3.8	0.30	2.0	0.58	1.8	27
MF-2720	2600	3.9	0.29	2.4	0.51	1.5	33
MF-2721	2485	4.2	0.30	3.1	0.60	1.2	7
MF-2722	2420	4.3	0.31	2.5	0.70	1.8	19
MF-2723	2375	4.5	0.28	2.9	0.64	1.6	16
MF-2724	2215	4.7	0.31	3.3	0.61	1.4	3
MF-2725	2140	5.2	0.33	1.9	0.57	3.3	10
MF-2725a	2140	4.9	0.47	3.0	0.41	1.9	16
MF-2727	2100	5.3	0.47	3.0	1.21	2.3	7
MF-2729	2075	5.5	0.36	2.8	0.53	2.7	25
MF-2753	2045	5.6	0.49	2.4	0.87	3.2	22
MF-3178	2030.3	3.8	0.35	2.1	0.58	1.7	62
MF-3179	2030	4.1	0.54	1.6	0.49	2.5	35
MF-2754	2025	5.0	0.33	2.9	0.53	2.1	16
MF-3180	2020	4.3	0.42	2.0	0.39	2.4	71
MF-3181	2015.2	5.9	0.49	2.3	0.38	3.6	15
MF-3182	2015	4.2	0.67	2.3	0.38	1.9	8
MF-3183	2000	4.6	0.45	2.5	0.47	2.2	6
MF-2755	1990	5.2	0.31	3.6	0.50	1.6	7
MF-2756	1990	4.5	0.14	4.0	0.36	0.6	6
MF-2757	1945	4.9	0.25	3.8	0.64	1.1	7
MF-2757a	1945	4.5	0.28	3.0	0.42	1.5	24
MF-2757b	1945	5.1	0.42	3.2	0.48	1.9	15
MF-2761	1700	5.8	0.55	3.3	0.84	2.5	3
MF-2762	1635	5.5	1.17	3.3	1.05	2.2	11

x=mean value; s=standard deviation; n=number of measurements.

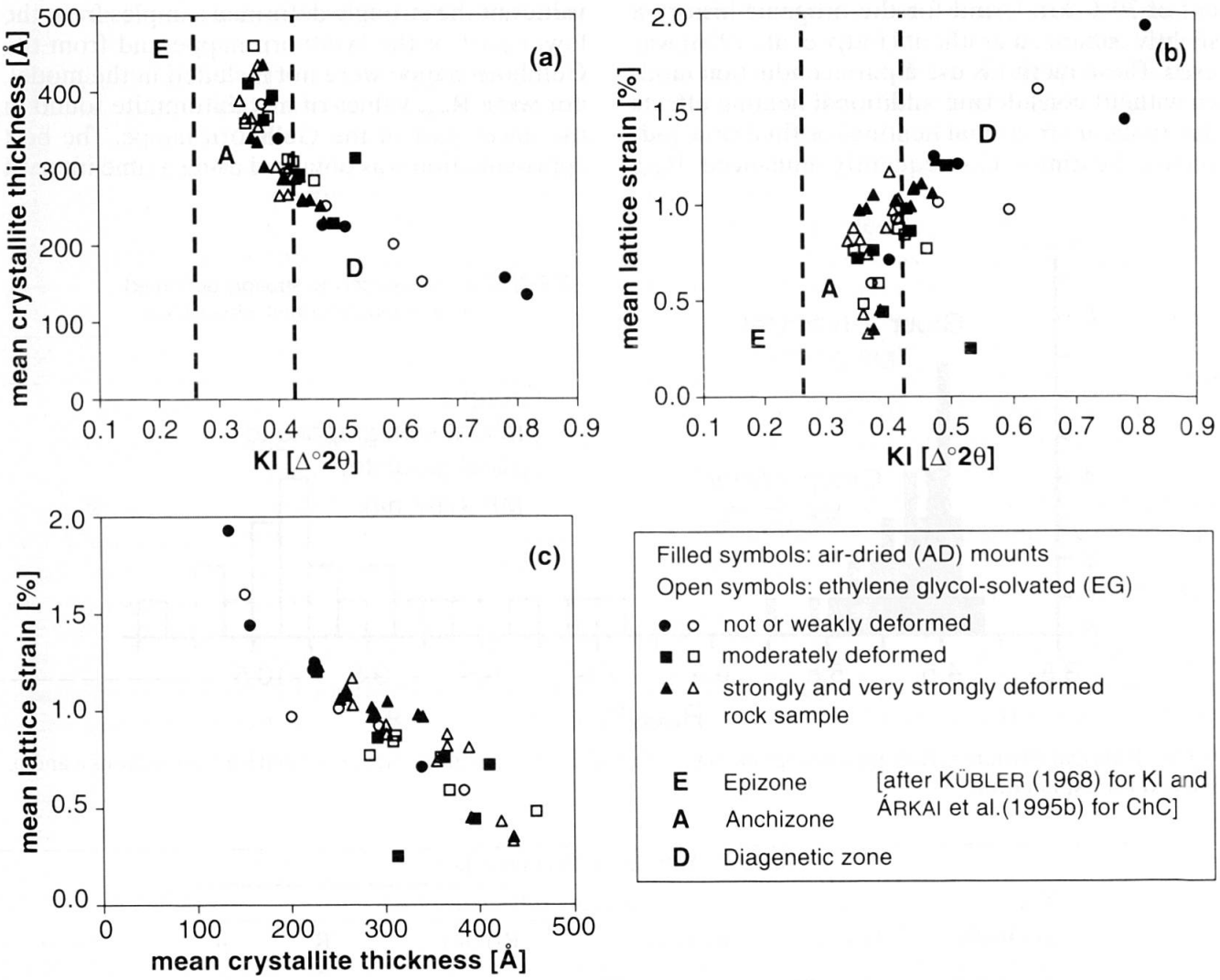

Fig. 7 Relationships between Kübler index and apparent mean crystallite size (a), mean lattice strain (b) and between mean crystallite size and lattice strain (c) of illite-muscovite.

Table 5 K–Ar ages obtained on illite-muscovite-rich, 0.1–2 μm grain-size fraction samples.

sample	K [weight-%]	^{40}Ar(rad) [ccSTP/g]	$\frac{^{40}\text{Ar(rad)}}{^{40}\text{Ar(total)}}$	Age [Ma ± 1σ]
MF-2719	4.07	1.436×10^{-5}	0.800	88.6 ± 3.4
MF-2720	4.22	1.449×10^{-5}	0.814	86.2 ± 3.3
MF-2721	5.87	1.458×10^{-5}	0.773	62.8 ± 2.4
MF-2722	4.71	1.677×10^{-5}	0.793	89.4 ± 3.4
MF-2723	4.79	1.440×10^{-5}	0.763	75.7 ± 3.0
MF-2724	3.14	7.009×10^{-6}	0.762	56.5 ± 2.2
MF-2725	4.42	1.008×10^{-5}	0.743	57.7 ± 2.2
MF-2727	3.81	9.789×10^{-6}	0.582	64.9 ± 2.6
MF-2729	3.98	1.138×10^{-5}	0.725	72.1 ± 2.8
MF-2753	4.22	1.036×10^{-5}	0.821	62.1 ± 2.4
MF-2754	3.36	7.267×10^{-6}	0.493	54.8 ± 2.3
MF-2755	4.03	6.242×10^{-6}	0.612	39.4 ± 1.6
MF-2756	4.40	8.470×10^{-6}	0.541	48.9 ± 2.0
MF-2757	4.79	6.502×10^{-6}	0.474	34.6 ± 1.5
MF-2760	5.86	9.573×10^{-6}	0.685	41.5 ± 1.7
MF-2761	4.91	7.136×10^{-6}	0.572	37.1 ± 1.5
MF-2762	5.06	6.033×10^{-6}	0.545	30.4 ± 1.3

of 2–5 Ma close to peak temperature. The model proposing a post-nappe metamorphism is presented with a bold gray line in Fig. 5. In this case, the modeled coalification gradient is the product of a (now missing) overburden of 12 km and a temperature gradient of 33 °C km^{-1}. This model is in agreement with the conditions found in the eastern vicinity of the profile studied, in the nappes forming the Kandersteg section (FREY et al., 1980; FREY and FERREIRO MÄHLMANN, 1999). However, the pattern of a downward increase of metamorphic grade with structural depth is in conflict with the metamorphic inversion pattern and the folded KI-VR zones in the northeast (Prealps, Fig. 1) and to the west of the Kandersteg section (MULLIS, 1976; KÜBLER et al., 1979; MOSAR, 1988; BURKHARD and GOY-EGGENBERGER, 2001). When the enhanced R_{max} values of highly strained rocks were also included, a higher thermal gradient (37 °C km^{-1}) would correspond to the Wildhorn and Gellihorn nappes, and a metamorphic inversion should have been supposed at the boundary between the Gellihorn and Doldenhorn nappes. However, VR data from the Doldenhorn nappe are insufficient to constrain a reliable trend, though we cannot rule out the possibility of "transported metamorphism" (FREY, 1988).

K–AR ISOTOPE GEOCHRONOLOGY

New K–Ar dates determined on illite-muscovite-rich, 0.1–2.0 μm grain-size fractions are given in Table 5. The age values vary strongly between ca. 90 and 30 Ma, showing a downward decreasing trend that is disturbed mainly at the nappe boundaries. Hence, the investigated parts of the three nappes differ from each other also in their K–Ar ages. In the Wildhorn nappe the K–Ar dates range between 89.4 and 56.5 Ma, with the lowest age values near the boundary between the Wildhorn and Gellihorn nappes. A local age de-

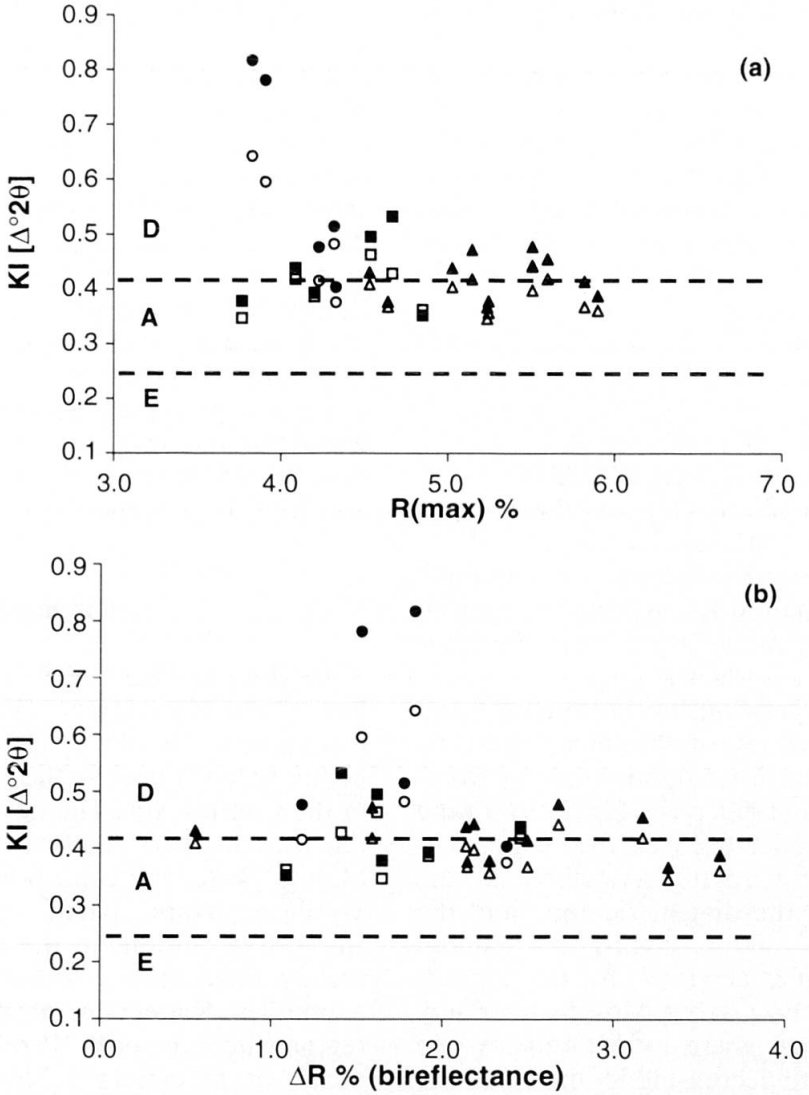

Fig. 8 Vitrinite reflectance vs. Kübler index. Symbols as in Fig. 2.

crease is observed also at about 2500 m a.s.l. in sample MF-2721 with an anomalously low KI value. Our K–Ar dates vary between 72.1 and 54.8 Ma in the Gellihorn nappe, displaying lower values near the upper and especially the lower nappe boundaries. However, the ages obtained from the Gellihorn samples are higher than those of the over- and underlying surroundings. As compared with the hangingwall nappes, the Doldenhorn nappe shows lower K–Ar dates, and these scatter between 41.5 and 30.4 Ma.

CORRELATION OF CLAY-MINERAL AND ORGANIC PARAMETERS

Differences between KI values measured on air-dry (AD) and glycolated (EG) mounts, being significant for diagenetic samples, decrease with decreasing KI (Fig. 2). However, small differences between KI(AD) and KI(EG) are also found in anchizonal samples, due to the presence of subordinate smectitic mixed-layers. These observations reflect the well-known trend of smectite-to-illite transformation observed during diagenesis and incipient metamorphism of pelitic rocks (for recent reviews see MERRIMAN and PEACOR, 1999; MERRIMAN and FREY, 1999). Consequently, the apparent mean crystallite thickness values of illite-muscovite calcuated from XRD line-profiles of the glycolated mounts are generally larger, whereas their lattice strain values are smaller than for air-dry mounts (Fig. 3).

Significant positive linear correlations exist between KI and chlorite "crystallinity" indices, namely:

r[KI, AD vs. ChC(001), AD] = 0.61,
r[KI, EG vs. ChC(001), EG] = 0.55,
r[KI, AD vs. ChC(002), AD] = 0.72, and
r[KI, EG vs. ChC(002), EG] = 0.76.

The range of changes in chlorite "crystallinity" indices is smaller than in KI, agreeing fairly well with observations on metaclastic rocks from other terranes (ÁRKAI et al., 1995b).

The hyperbolic relationship between KI and mean crystallite thickness of illite-muscovite (Fig. 7a) is very similar to those summarized by MERRIMAN and PEACOR (1999, p. 49, Fig. 2.19). In the profile from the Kandersteg area, the mean thickness of the illite-muscovite crystallites at the boundary between the diagenetic zone and the anchizone is ca. 250–300 Å, slightly less than determined by ÁRKAI et al. (1997) for the Tertiary flysch samples of the Glarus Alps, Switzerland, but within the range given by MERRIMAN and PEACOR (1999). With decreasing KI the mean lattice strain of illite-muscovite decreases, but this relation has only a low level of significance (Fig. 7b). There is a well constrained negative correlation between the mean crystallite thickness and mean lattice strain values of illite-muscovite (Fig. 7c).

Some samples in the Gellihorn nappe show striking differences in the "crystallinity", the apparent mean crystallite thickness and mean lattice strain values measured on air-dry and glycolated mounts (Figs. 2, 3 and 4). These differences are due to elevated amounts of smectitic mixed-layers in illite and chlorite. The mixed-layer minerals are thought to be post-metamorphic alteration products, independent of metamorphic grade.

Figure 8 displays the relationships between illite "crystallinity" and vitrinite reflectance. Triangle-shaped distributions suggest that the scatter in R_{max} and ΔR increases with decreasing KI (Figs. 8a–b). With increasing R_{max} the scatter in KI decreases (Fig. 8a), while the scatter in KI is the largest at about 1.5–1.9% ΔR (Fig. 8b). These distributions are different from the general trends of KI-VR relations in burial tectonic settings (for extensive reviews see KISCH, 1983, 1987; MERRIMAN and FREY, 1999). As shown in Fig. 8, samples with diagenetic KI may have VR values as high as 5.6% R_{max} with bireflectance >3.0%. Samples with the KI values roughly corresponding to the boundary between the diagenetic zone and the anchizone show scatter in VR around 4.0 and 5.7% R_{max}, and 0.5 and 2.5% ΔR, respectively. Much lower VR values, between 2.5 to 3.3% R_{max}, are characteristic of this boundary for specific Penninic and Austroalpine nappes in the Alps (FREY et al., 1980, FERREIRO MÄHLMANN, 1995, 2001). In the neighbouring Kien valley profile, FREY et al. (1980) found that the onset and the end of the anchizone determined on the basis of KI correspond to 3.0 and 5.7% R_{max}, respectively.

Discussion

According to FREY et al. (1980) and FREY and FERREIRO MÄHLMANN (1999) the diagenetic/metamorphic grade increases from structurally higher to lower units in the Helvetic nappe edifice of the Central Alps. The new KI and ChC data in the present work confirm this general pattern. Mainly diagenetic conditions were found in the Wildhorn nappe, partly diagenetic, partly anchizonal conditions in the Gellihorn nappe and mainly anchizonal conditions in the Doldenhorn nappe. The Kandersteg area is at the limit of the region where the post-"Pizol" and syn-"Calanda" phase of metamorphic overprint is well constrained (FREY et al., 1976; HOEFS and FREY, 1976;

KAHR et al., 1996); this is post-kinematic to nappe thrusting. However, as shown by Figs. 2, 3, and 5, the general trend of downward increasing metamorphic grade is considerably disturbed near the thrust planes, especially in the Gellihorn and the upper part of the Doldenhorn nappes. The possible reasons of these disturbances are discussed in the following paragraphs.

In contrast to the KI-VR relation in many low-grade metamorphic orogenic settings, considerable retardation of phyllosilicate reaction progress, as compared to organic maturity, is demonstrated in the Kandersteg profile. However, relatively high values of VR (R_{max} and R_{random}) in some Gellihorn samples from the Kien valley profile (Berner Oberland) was already noted by FREY et al. (1980). KISCH (1980) also measured high VR in samples with "diagenetic" KI from other localities of the Wildhorn nappe in the Kandergrund area, but no satisfactory explanation was available. Enhanced VR relative to KI and other clay mineral parameters used for determining metamorphic grade remain to be explained also for the eastern part of the Helvetic domain (ERDELBROCK, 1994; RAHN et al., 1994). The following reasons for this anomalous relation between VR and KI found in the Kandersteg area are considered:

(a) Line-broadening (KI-increase) due to Na- or Ca-white micas: while these may be present in a few samples as traces (Table 2), they cannot explain the anomaly, because chlorite "crystallinity" shows the same effect.

(b) Isolation of phyllosilicate grains by finely dispersed organic matter: This may cause appreciable delay in phyllosilicate aggradation (for review, see FREY, 1987), but neither the amount of organic matter nor its dispersion differ considerably from those of common metaclastic rocks of other localities. In addition, microscopic observations show no shield covering of organic matter (bituminite) around phyllosilicates either. Therefore, this factor can be excluded.

(c) A relatively short-lived (regional or local) thermal event, which may produce retardation in phyllosilicate "crystallinity" as compared to coal rank: Considerable differences exist between reaction rates of phyllosilicates and of coalification process, the latter being much more rapid (STADLER and TEICHMÜLLER, 1971; WOLF, 1975; for an extensive critical review see KISCH, 1987). In the profile studied, thermal modeling gave the best approximation using a time interval of 2–5 Ma close to peak temperature; geologically, this does represent short-term heating. A relatively short-lived regional thermal event has also been postulated but not proven by RAHN et al. (1995) for the region of Lake Lucerne and east of this area. In the Kandersteg profile, the brevity of orogenic heating is proposed as the principal cause of retardation in phyllosilicate reaction progress. In the mylonitic zone of the Gellihorn nappe and in the micro-shear zones of the Doldenhorn nappe, this retardation is much more pronounced than in the Wildhorn nappe, because strain has further elevated the maximum reflectance of vitrinite due to pre-graphitic processes, as indicated by the increase in structural ordering (PETROVA et al., 2002 and FERREIRO MÄHLMANN et al., 2002).

(d) Phyllosilicate retrogression caused by hydrothermal fluids: In the permeable cataclastic-mylonitic zone of the Gellihorn nappe, fluid flow caused intense chloritization and formation of swelling interstratifications. Similar phenomena were described by FERREIRO MÄHLMANN (2001) for the Austroalpine-Penninic tectonic contact in Eastern Switzerland. However, hydrothermal phyllosilicate degradation is not regarded a general phenomenon affecting the entire profile studied.

(e) Tectonic shear strain: As discussed in general by TEICHMÜLLER (1987) and suggested by SUCHÝ et al. (1997) for the profile in question, deformation might effectively enhance coalification and graphitization especially at higher ranks (anthracite stage and higher). SUCHÝ et al. (1997) speculated that frictional heating associated with localized shear had contributed to advanced coalification and graphitization. Tectonic shear strain also promotes phyllosilicate reaction progress (for a recent review see MERRIMAN and FREY, 1999).

Considering the thin-skin nappe tectonics of the Kandersteg area, tectonic shear-strain provides an acceptable explanation for the organic maturity relations, even if quantitative physical parameters of shear strain are lacking, both for the thrust zones separating the nappes and the meso- and micro-scale shear zones (e.g. ENGLAND and MOLNAR, 1993). Differences in shear-strain correlate with inhomogeneities in organic maturity found in various portions of the samples studied and also within the profile in general (see also SUCHÝ et al., 1997).

It seems plausible that short-lived tectonic shear strain (and the related frictional heat) localized in micro-, meso- and outcrop-scale zones affected organic maturation processes far more directly than it influenced reaction progress of phyllosilicates. While the diversity of organic maturity parameters within each sample refers to micro-scale variations in shear-related progress of organic maturation, phyllosilicate "crystallinity", crystallite thickness and lattice strain values express only weighted averages of the state the

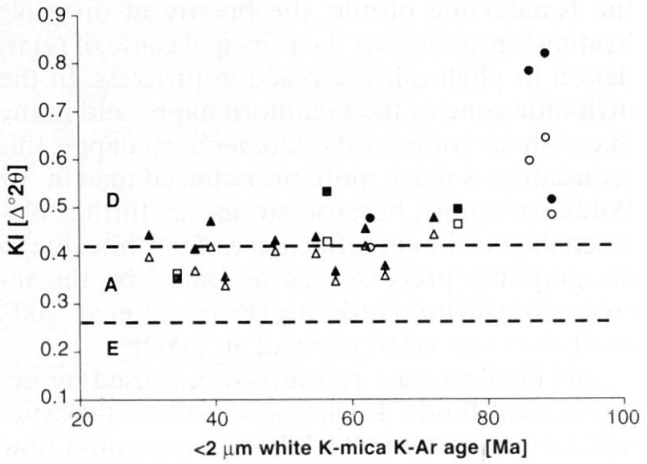

Fig. 9 Relation between Kübler index and K–Ar age of clay-size white K-mica. Symbols as in Fig. 2.

phyllosilicates reached during their disequilibrium transformations. This may explain why correlations between organic and inorganic maturity parameters are as weak as shown in Fig. 8.

However, the deviations from the general trend of a downward increase in metamorphic grade, as expressed in the phyllosilicate characteristics, are predominantly related to local increases in tectonic shear strain. In the lower parts of Figs. 2, 3, and 4, the sections near the main overthrust planes and the whole Gellihorn section of the studied profile are enlarged. In the lower part of the Wildhorn nappe, as well as in the whole Gellihorn nappe, the apparent metamorphic grade increases towards the nappe boundaries, where shear strain was localized. The opposite trend, a decrease in grade, is found in the upper part (near the thrust) of the Doldenhorn nappe, the metamorphic grade of which is higher (mostly anchizonal) than in the top two nappes. Thus, in high-level shear zones the (prograde or retrograde) deviation also depends on the diagenetic-metamorphic grade the samples reached prior to thin-skin thrusting. Shear-related recrystallization may result in smaller KI and ChC values, smaller lattice strain and larger crystallite thickness, showing higher apparent grades in diagenetic and lower anchizonal rocks, while the same tectonic process may lead to retrogression in case of higher-grade (anchi- and epizonal) rocks.

The strong scatter in both general (burial-related) and local (shear-related) phyllosilicate trends in the studied profile is related to the superposition of additional effects. Among these, the effect of detrital, inherited phyllosilicates can be traced using K–Ar isotope geochronological data of clay-size white mica (Table 5). The K–Ar system in illite-muscovite was almost completely reset only in some anchizonal samples of the Doldenhorn nappe. Considering that the Alpine metamorphism acted between ca. 35 and 15 Ma (BURKHARD, 1988; HUON et al., 1994), this result is in agreement with HUNZIKER et al. (1986), who showed that complete resetting of the <2.0 μm illite-muscovite requires an integrated temperature-time effect of 260 ± 20 °C during 10 ± 5 Ma. All of the K–Ar dates obtained from the Wildhorn and Gellihorn nappes may be interpreted as mixed ages devoid of well-defined geological meaning, because the effects of detrital, inherited K-white micas, newly-formed diagenetic illites and Alpine metamorphic illite-muscovites are superposed in various proportions. The moderate positive linear correlation ($r = 0.69$, $n = 17$) between KI and K–Ar dates implies increasing partial rejuvenation of illite-muscovite with increasing grades at late diagenetic and low-T anchizonal conditions (Fig. 9), a common observation of incipient metamorphism (HUNZIKER, 1987).

Conclusions

New KI and ChC data compared with previous and new organic petrographic and microstructural observations from the Kandersteg profile confirm the general trend of changes in metamorphic grade in the Helvetic zone of the Central Alps described by FREY et al. (1980): Grades tend to increase from tectonically higher to lower nappes. In the section studied, the topmost (Wildhorn) nappe shows predominantly diagenetic, the middle (Gellihorn) nappe partly diagenetic, partly anchizonal, and the lower (Doldenhorn) nappe mainly anchizonal conditions. This pattern corresponds to normal tectonic burial caused by the overriding Penninic nappes.

Significant delay or retardation of reaction progress of phyllosilicates is demonstrated in the Kandersteg profile, as compared with organic maturity (VR, graphitization) and microstructural features described by SUCHÝ et al. (1997) and in this study. Evaluating the potential causes, geologically short-lived conditions near metamorphic peak temperature combined with the effects of tectonic shear strain (possibly accompanied by localized frictional heating) seems to be the most viable explanation in the Kandersteg profile. The effects of fluid-controlled chloritization in the cataclastic-mylonitic zone of the Gellihorn nappe are noted. Phyllosilicate retrogression by fluid alteration was followed by hydrocarbon migration. Fluid flow during cooling was again localized along the same tectonic horizons.

The general trend of metamorphic grade increasing downwards was considerably disturbed

in the vicinity of nappe boundaries and also within the Wildhorn and Doldenhorn nappes. High tectonic shear strain concentrated at nappe boundaries, as well as lithological boundaries within the nappes, resulted in a local decrease of KI and ChC, hence an increase of grade and apparent mean crystallite size of illite-muscovite and chlorite. Thus, high shear strains promoted not only organic maturity (coalification and graphitization), but – to a lesser extent – this also enhanced phyllosilicate reaction progress. By contrast, signs of possible strain-related retrogression of illite-muscovite were found in the uppermost part of the Doldenhorn nappe. Seemingly, the prograde or retrograde nature of the shear-related alteration depend also on the diagenetic-metamorphic grade the rocks had reached prior to thin-skin thrust tectonics.

K–Ar dates measured on clay-size K-white mica fractions are in agreement with the conclusions drawn from the illite "crystallinity" values. Decreasing mixed ages with decreasing KI provides an example of increasing, incomplete rejuvenation with advancing grade.

Acknowledgements

The present work is a part of the projects Nrs. 20-50'652.97 and 20-50'6842.99 "Studies in Very Low-Grade Metamorphism" headed by M.F. and supported by the Schweizerischer Nationalfonds zur Förderung der Wissenschaftlichen Forschung. P.Á. and K.B. acknowledge financial support from the Hungarian National Scientific Research Fund (OTKA), Budapest, for metamorphic petrological research including all of the XRD studies (program Nr. T-035050 to P.Á.) and for isotope geochronological studies (program Nr. T-029897 to K.B.). The organic petrographic study was supported by the Grant Agency of the Czech Academy of Sciences (S3046004). Thanks are due to Mrs. Olga Komoróczy, Csaba M. Sándor and Ms. Katalin Temesvári and Noémi Keresztes (Laboratory for Geochemical Research, Hung. Acad. Sci., Budapest) for their technical assistance. The authors are grateful to Dr. Fernando Nieto (Granada, Spain) and Dr. Laurence N. Warr (Heidelberg, Germany) for critically reviewing and correcting an earlier version of this work, and are deeply indebted to Prof. Martin Engi (Bern) and Dr. Susanne Th. Schmidt (Geneva, Switzerland) for reviewing the manuscript and providing the additional rock samples and field notes of Professor Martin Frey for further analytical work after his tragic death.

References

ÁRKAI, P., BALOGH, K. and DUNKL, I. (1995a): Timing of low-temperature metamorphism and cooling of the Paleozoic and Mesozoic formations of the Bükkium, innermost Western Carpathians, Hungary. Geol. Rundschau 84, 334–344.

ÁRKAI, P., BALOGH, K. and FREY, M. (1997): The effects of tectonic strain on crystallinity, apparent mean crystallite size and lattice strain of phyllosilicates in low-temperature metamorphic rocks. A case study from the Glarus overthrust, Switzerland. Schweiz. Mineral. Petrogr. Mitt. 77, 27–40.

ÁRKAI, P., SASSI, F.P. and SASSI, R. (1995b): Simultaneous measurements of chlorite and illite crystallinity: a more reliable geothermometric tool for monitoring low- to very low-grade metamorphism in metapelites. A case study from Southern Alps (NE. Italy). Eur. J. Mineral. 7, 1115–1128.

ÁRKAI, P., MERRIMAN, R.J., ROBERTS, B., PEACOR, D.R. and TÓTH, M. (1996): Crystallinity, crystallite size and lattice strain of illite-muscovite and chlorite: comparison of XRD and TEM data for diagenetic to epizonal pelites. Eur. J. Mineral. 8, 1119–1137.

BUCHER, K. and FREY, M. (1994): Petrogenesis of metamorphic rocks. Springer-Verlag, Berlin, Heidelberg, 308 pp.

BURKHARD, M. (1988): L'Helvétique de la bordure occidentale du massif de l'Aar (évolution tectonique et métamorphique). Eclogae geol. Helv. 81, 63–114.

BURKHARD, M. and BADERTSCHER, N. (2001): Finite strain has no influence on the illite crystallinity of tectonized Eocene limestone breccias of the Morcles nappe, Swiss Alps. Clay Min. 36, 171–180.

BURKHARD, M. and GOY-EGGENBERGER, D. (2001): Near-vertical iso-illite-crystallinity surfaces crosscut the recumbent fold structure of the Morcles nappe, Swiss Alps. Clay Min. 36, 159–170.

ENGLAND, P. and MOLNAR, P. (1993): The interpretation of inverted metamorphic isograds using simple physical calculations. Tectonics 12, 145–157.

ERDELBROCK, K. (1994): Diagenese und schwache Metamorphose im Helvetikum der Ostschweiz (Inkohlung und Illit "Kristallinität). PhD thesis Rhein-Westf. Techn. Hochschule Aachen, 219 pp.

FERREIRO MÄHLMANN, R. (1995): Das Diagenese-Metamorphose-Muster von Vitrinitreflexion und Illit-"Kristallinität" in Mittelbünden und im Oberhalbstein. Teil 1: Bezüge zur Stockwerktektonik. Schweiz. Mineral. Petrogr. Mitt. 75/1, 85–122.

FERREIRO MÄHLMANN, R. (1996): Das Diagenese-Metamorphose-Muster von Vitrinitreflexion und Illit "Kristallinität" in Mittelbünden und im Oberhalbstein. Teil 2: Korrelation kohlenpetrographischer und mineralogischer Parameter. Schweiz. Mineral. Petrogr. Mitt. 76/1, 23–46.

FERREIRO MÄHLMANN, R. (2001): Correlation of very low grade data to calibrate a thermal maturity model in a nappe tectonic setting, a case study from the Alps. Tectonophysics 334, 1–33.

FERREIRO MÄHLMANN, R., PETROVA, T., PIRONON, J., STERN, W.B., GHANBAJA, J., DUBESSY, J. and FREY, M. (2002): Transmission electron microscopy study of carbonaceous material in a metamorphic profile from diagenesis to amphibolite facies (Bündnerschiefer, Eastern Switzerland). Schweiz. Mineral. Petrogr. Mitt. 82, 253–272.

FREY, M. (1986): Very low-grade metamorphism of the Alps – an introduction. Schweiz. Mineral. Petrogr. Mitt. 66, 13–27.

FREY, M. (1987): Very low-grade metamorphism of clastic sedimentary rocks. In: FREY, M. (ed.): Low Temperature Metamorphism. Blackie, Glasgow and London, 9–58.

FREY, M. (1988): Discontinuous inverse metamorphic zonation, Glarus Alps, Switzerland: evidence from illite "crystallinity" data. Schweiz. Mineral. Petrogr. Mitt. 68, 171–183.

FREY, M. and FERREIRO MÄHLMANN, R. (1999): Alpine metamorphism of the Central Alps. Schweiz. Mineral. Petrogr. Mitt. 79, 135–154.

FREY, M., JÄGER, E. and NIGGLI, E. (1976): Gesteinsmetamorphose im Bereich der Geotraverse Basel–Chiasso. Schweiz. Mineral. Petrogr. Mitt. 56, 649–659.

FREY, M., TEICHMÜLLER, M., TEICHMÜLLER, R., MULLIS, J., KÜNZI, B., BREITSCHMID, A., GRUNER, U. and SCHWIZER, B. (1980): Very low-grade metamorphism in external parts of the Central Alps: Illite crystallinity, coal rank and fluid inclusion data. Eclogae geol. Helv. 73, 173–203.

HOEFS, J. and FREY, M. (1976): The isotopic composition of carbonaceous matter in a metamorphic profile from the Swiss Alps. Geochim. Cosmochim. Acta 40, 945–951.

HUNZIKER, J.C. (1987): Radiogenic isotopes in very low-grade metamorphism. In: FREY, M. (ed.): Low Temperature Metamorphism. Blackie, Glasgow and London, 200–226.

HUNZIKER, J., FREY, M., CLAUER, N., DALLMEYER, R.D., FRIEDRICHSEN, H., FLEHMIG, W., HOCHSTRASSER, K., ROGGWILER, P. and SCHWANDER, H. (1986): The evolution of illite to muscovite: mineralogical and isotopic data from the Glarus Alps, Switzerland. Contrib. Mineral. Petrol. 92, 157–180.

HUON, S., BURKHARD, M. and HUNZIKER, J. (1994): Mineralogical, K–Ar, stable and Sr isotope systematics of K-white micas during very low-grade metamorphism of limestones (Helvetic nappes, western Switzerland). Chem. Geol. Isotope Geosci. Sect. 113, 347–376.

KAHR, G., FREY, M. and MADSEN, F.T. (1996): Thermoanalytical dehydroxilation of clays and combustion of organic compounds in a prograde metamorphic Liassic black shale formation, Central Swiss Alps. Schweiz. Mineral. Petrogr. Mitt. 76, 165–173.

KISCH, H.J. (1980): Illite crystallinity and coal rank associated with lowest-grade metamorphism of the Taveyanne greywacke in the Helvetic zone of the Swiss Alps. Eclogae geol. Helv. 73, 753–777.

KISCH, H.J. (1983): Mineralogy and petrology of burial diagenesis (burial metamorphism) and incipient metamorphism in clastic rocks. In: LARSEN, G. and CHILINGAR, G.V. (eds): Diagenesis in Sediments and Sedimentary rocks, 2. Elsevier, Amsterdam, 289–493.

KISCH, H.J. (1987): Correlation between indicators of very low-grade metamorphism. In: FREY, M. (ed.): Low Temperature Metamorphism. Blackie, Glasgow and London, 227–300.

KISCH, H.J. (1989): Discordant relationship between degree of very-low-grade metamorphism and the development of slaty cleavage. In: DALY, J.S., CLIFF, R.A. and YARDLEY, B.W.D. (eds): Evolution of metamorphic belts. Geol. Soc. London Spec. Publ. 43, 173–185.

KISCH, H.J. (1991): Development of slaty cleavage and degree of very-low-grade metamorphism: a review. J. Metamorphic Geol. 9, 735–750.

KÜBLER, B. (1968): Evaluation quantitative du métamorphisme par la cristallinité de l'illite. Bull. Centre Rech. Pau - S.N.P.A. 2, 385–397.

KÜBLER, B., PITTION, J.-L., HÉROUX, Y., CHAROLLAIS, J. et WEIDMANN, M. (1979): Sur le pouvoir réflecteur de la vitrinite dans quelques roches du Jura, de la Molasse et des Nappes préalpines, helvétiques et penniques. Eclogae geol. Helv. 72, 347–373.

LANGFORD, J.I. (1978): A rapid method for analysing the breadth of diffraction and spectral lines using the Voigt function. J. Appl. Cryst. 11, 10–14.

MERRIMAN, R.J. and FREY, M. (1999): Patterns of very low-grade metamorphism in metapelitic rocks. In: FREY, M. and ROBINSON, D (eds): Low-Grade Metamorphism. Blackwell Science, Oxford, 61–107.

MERRIMAN, R.J. and PEACOR, D.R. (1999): Very low-grade metapelites: mineralogy, microfabrics and measuring reaction progress. In: FREY, M. and ROBINSON, D. (eds): Low-Grade Metamorphism. Blackwell Science, Oxford, 10–60.

MOSAR, J. (1988): Métamorphisme transporté dans les Préalpes. Schweiz. Mineral. Petrogr. Mitt. 68, 77–94.

MULLIS, J. (1976): Die Quartzkristalle des Val d'Illiez – Zeugen spätalpiner Bewegungen. Eclogae geol. Helv. 69, 343–357.

PETROVA, T.V., FERREIRO MÄHLMANN, R., STERN, W.B. and FREY, M. (2002): Application of combustion and TGA-DTA analysis to the study of metamorphic organic matter. Schweiz. Mineral. Petrogr. Mitt. 82/1, 33–53.

PFIFFNER, O.A. (1986): Evolution of the north Alpine foreland basin in the Central Alps. Spec. Public. Int. Assoc. Sediment. 8, 219–228.

RAHN, M., MULLIS, J., ERDELBROCK, K. and FREY, M. (1994): Very low-grade metamorphism of the Taveyanne greywacke, Glarus Alps, Switzerland. J. Metamorphic Geol. 12, 625–641.

RAHN, M., MULLIS, J., ERDELBROCK, K. and FREY, M. (1995): Alpine metamorphism in the North Helvetic Flysch of the Glarus Alps, Switzerland. Eclogae geol. Helv. 88, 157–178.

RAHN, M., HURFORD, A.J. and FREY, M. (1997): Rotation and exhumation of a thrust plane: Apatite fission track data from the Glarus thrust, Switzerland. Geology 25/7, 599–602.

STADLER, G. and TEICHMÜLLER, R. (1971): Zusammenfassender Überblick über die Entwicklung des Bramscher Massivs und des Niedersächsischen Tektogens. Fortschr. Geol. Rheinl. Westf. 18, 547–564.

STEIGER, R.H. and JÄGER, E. (1977): Subcommission on geochronology: convention on the use of decay constants in geo- and cosmochronology. Earth Planet. Sci. Lett. 12, 359–362.

SUCHÝ, V., FREY, M. and WOLF, M. (1997): Vitrinite reflectance and shear-induced graphitization in orogenic belts: A case study from the Kandersteg area, Helvetic Alps, Switzerland. Int. J. Coal Geol. 34, 1–20.

SWEENEY, J.J. and BURNHAM, A.K. (1990): Evaluation of a simple model of vitrinite reflectance based on chemical kinetics. Amer. Assoc. Petrol. Geol. Bull., 74/10, 1559–1570.

TEICHMÜLLER, M. (1987): Organic material and very low-grade metamorphism. In: FREY, M. (ed.): Low Temperature Metamorphism. Blackie, Glasgow and London, 114–161.

TRÜMPY, R. (1980): Geology of Switzerland, Part A. Wepf and Co. Publishers, Basel, New York, 104 pp.

WARR, L.N., GREILING, R.O. and ZACHRISSON, E. (1996): Thrust-related very low grade metamorphism in the marginal part of an orogenic wedge, Scandinavian Caledonides. Tectonics 15, 1213–1229.

WOLF, M. (1975): Über die Beziehungen zwischen Illit-Kristallinität und Inkohlung. N. Jb. Geol. Paläont. Mh. 1975, 437–447.

ZWAHLEN, P. (1986): Die Kandertal-Störung, eine transversale Diskontinuität im Bau der Helvetischen Decken. Unpubl. PhD thesis, Bern University, 105 pp.

ZWAHLEN, P. (1993): Das Bundstock-Element, eine diskontinuierliche helvetische Teildecke an der Kandertal-Störung. Eclogae geol. Helv. 86, 65–86.

Manuscript received December 7, 2001; revision accepted June 11, 2002.
Editorial handling: M. Engi